

## Two-Electron Linear Intersubband Light Absorption in a Biased Quantum Well

J. Dafi, M. E. Raikh<sup>a</sup>, and T. V. Shahbazyan<sup>b</sup><sup>a</sup>Department of Physics, University of Utah, Salt Lake City, UT 84112<sup>b</sup>Department of Physics, Jackson State University, Jackson, MS 39217

We point out a novel manifestation of many-body correlations in the linear optical response of electrons confined in a quantum well. Namely, we demonstrate that along with conventional absorption peak at frequency  $\omega$  close to intersubband energy  $\omega_0$ , there exists an additional peak at frequency  $\omega \approx 2\omega_0$ . This new peak is solely due to electron-electron interactions, and can be understood as excitation of two electrons by a single photon. The actual peak lineshape is comprised of a sharp feature, due to excitation of pairs of intersubband plasmons, on top of a broader band due to absorption by two single-particle excitations. The two-plasmon contribution allows to infer intersubband plasmon dispersion from linear absorption experiments.

**Introduction** | Intersubband absorption of light in a quantum well (QW) is studied theoretically and experimentally for more than two decades. Original motivation for such a close attention to this process was its crucial role in design of infrared detectors [1]. Lately, the interest in intersubband transitions is spurred by advances in fabrication of the quantum cascade lasers [2].

Within a single-electron description and in the absence of nonparabolicity, the intersubband absorption peak is infinitely narrow and positioned precisely at  $\omega = \omega_0$ , where  $\omega_0 = E_2 - E_1$  is the intersubband separation (see Fig. 1). As electron-electron interactions are switched on, the adequate language for the description of absorption becomes the excitations of intersubband plasmon (ISP) by light polarized perpendicular to the QW plane. Many-body origin of the absorption manifests itself in a shift of peak position up from  $\omega = \omega_0$  (depolarization shift), and a finite peak width even at zero temperature and in the absence of disorder. While the shift has been understood long ago [3, 4, 5], the interaction-induced broadening of the absorption line still remains a subject of debate. The peak lineshape was addressed in several recent studies that employed various approximate many-body schemes, and yielded lineshapes calculated numerically for particular sets of QW parameters [6, 7, 8, 9, 10, 11]. The lack of analytical description (even in the limit of weak interactions) reflects the fact that the peak lineshape is governed by very delicate correlations in 2D electron gas.

In the present paper we point out that, in addition to conventional intersubband absorption, there exists a distinctive interaction-induced effect, namely, two-particle linear absorption of light. Obviously, without interactions, one photon can excite only one electron from the lower to the upper subband. This is the case even in the presence of disorder that violates momentum conservation. Our main point is that interactions allow a photon with energy  $\omega \approx 2\omega_0$  to excite simultaneously two intersubband excitations (single-particle or collective). As a result, the absorption peak is comprised of a sharp feature originating from excitation of two ISPs on top of a broader band of two single-particle excitations. We show that absorption of a photon by two single-particle excitations can be captured perturbatively in the interaction

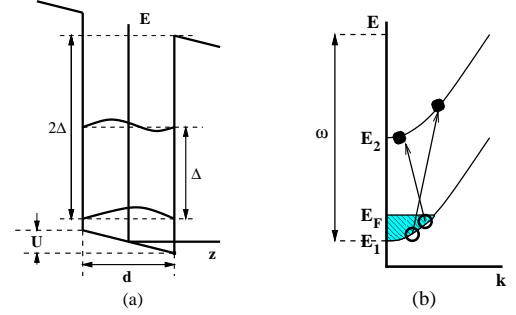


FIG. 1: (a) Two lowest size-quantization wave functions of a biased quantum well are shown schematically; for two-electron linear absorption, the incident photon energy must be close to  $2\omega_0$ . (b) Two-electron intersubband absorption in the lowest order of the perturbation theory.

strength. By contrast, in order to describe two-plasmon absorption, a nonperturbative approach is required. Such an approach is developed in this paper.

A remarkable feature of two-particle absorption is that the ISP dispersion  $\omega_{p1}(q)$  at finite momenta can be inferred from the peak shape. Indeed, with two finite-momentum ISPs in the initial state, the momentum conservation can be respected even though the momentum of an incident photon is negligible [12]. Another distinctive feature of the  $2\omega_0$  peak is its sensitivity to external bias,  $U$ , applied across QW; for a symmetric QW, the  $2\omega_0$  peak emerges only at finite  $U$  and grows as  $U^2$ .

**Formalism** | The proposed effect is most naturally described in diagrammatic language. The conventional absorption is represented by standard polarization bubble (see Fig. 2(a)). Dipole matrix elements  $z_{12} = \int \psi_1^* z \psi_2 dz$  in the vertices are responsible for promotion of an electron from subband 1 to subband 2 (see Fig. 1), where  $\psi_1, \psi_2$  are the size-quantization wavefunctions. Since the momentum of photon is negligibly small, the intersubband polarization operator is simply  $P_0(\omega) = \frac{N}{i(\omega - \omega_0)}$ , where  $N = \frac{k_F^2}{2\pi}$  is electron concentration and  $k_F$  is the Fermi momentum. We assume that the Fermi energy  $E_F = \frac{\hbar^2 k_F^2}{2m}$  is smaller than  $E_2 - E_1$  (here  $m$  is the electron

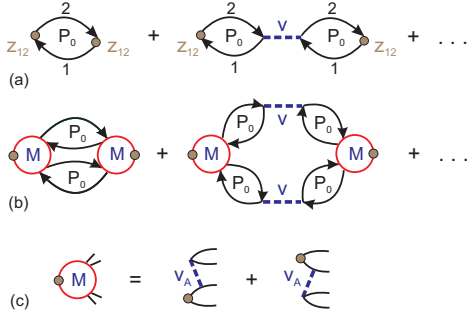


FIG. 2: Diagrammatic representation of single-particle absorption (a), two-particle absorption (b) and two-electron dipole matrix element (c).  $V_A$  stands for  $V_{1222}$  and  $V_{1211}$  in first and second diagram, respectively.

mass). As explained above, the adequate picture of absorption is excitation of ISP (rather than electron-hole pair). Diagrammatically (see Fig. 2(a)) this is accomplished by a standard RPA summation of polarization bubbles connected by intersubband Coulomb matrix element,  $V = V_{1212}(0)$ ; we adopt the standard definition of matrix elements

$$V_{ijkl}(q) = v_q \int dz dz' \phi_i(z) \phi_j(z') \phi_k(z) \phi_l(z - qz) e^{iqz} \quad (1)$$

where  $v_q = \frac{2e^2}{q}$  is the Fourier component of 2D Coulomb potential and  $\epsilon$  is the dielectric constant. For a rectangular well, we have  $V_{1212}(0) = \epsilon_0$ , where  $\epsilon_0 = m = \epsilon^2$  is the 2D density of states, while the dimensionless parameter  $\epsilon_0$  is given by

$$\epsilon_0 = \frac{10}{9} r_s \frac{P}{6E_F}; \quad (2)$$

where  $r_s = \frac{P}{2m} \frac{e^2}{\epsilon^2} = \frac{\epsilon^2}{k_F}$  is the interaction parameter. The RPA summation amounts to a replacement of  $P_0$  by the ISP propagator  $P_0(1 - V_{1212}P_0)^{-1}$ . It is important that at  $q = 0$  the propagator  $P_0(0) = \frac{N}{V_{1212}}$  has the same form as  $P_0(0)$  except for the depolarization shift of the pole position [3, 4, 5]. Thus, within RPA, the entire oscillator strength is simply transferred to ISP.

It is convenient to explain the novel absorption peak at  $\omega = 2$  by building on analogy to Fig. 2(a). The corresponding diagrams are presented in Fig. 2(b). The vertices  $M_q$  now stand for matrix elements that transform a photon into two intersubband electron-hole (e-h) pairs. Each electron (hole) propagator in Fig. 2(a) is now replaced by double line (one electron and one hole). All four lines begin (and end) at the same vertex.

It is obvious that, without interactions,  $M_q$  is identically zero. This is the case even in the presence of disorder and reflects the orthogonality of eigenstates in QW. Our prime observation is that interactions give rise to a finite  $M_q$ . In the lowest order in interactions, the diagram for  $M_q$  is shown in Fig. 2(c). The underlying virtual process can be described as follows. A photon with energy

$\omega = 2$  first creates an e-h pair by promoting an electron to the second subband. The electron from this pair subsequently undergoes intrasubband scattering, accompanied by excitation of intersubband e-h pair. The propagator of this pair is shown by the first double-line emerging from the vertex  $M_q$  in Fig. 2(b), while the second double-line corresponds to intrasubband-scattered photoexcited electron and photoexcited hole. Apparently, there is also a second contribution to  $M_q$ , originating from intrasubband scattering of the hole, as shown in Fig. 2(c).

We now turn to the higher-order diagram in Fig. 2(b). In higher orders in interactions, each double-line, that represented a propagating e-h pair in the lowest-order diagram, is now replaced by ISP propagator. Such a "dressing" is analogous to single-particle to collective excitation transformation in the usual absorption [see Fig. 2(a)]. Correspondingly, the absorption coefficient has a general form

$$\chi''(\omega)/\omega = \sum_q M_q^2 J(\omega; q); \quad (3)$$

(we omitted a frequency-independent factor), where the joint spectral function  $J(\omega; q)$  is given by a convolution

$$J(\omega; q) = \int \frac{dE}{2} 2 \text{Im}(\epsilon(E; q)) 2 \text{Im}(\epsilon(\omega - E; q)); \quad (4)$$

of two ISP propagators. Energy dependence of  $\epsilon(E; q)$  comes from the free-electron intersubband polarization,

$$P_0(E; q) = 2 \int \frac{dp}{(2\pi)^2} \frac{n_{1p}}{E + \epsilon_p - \epsilon_{p+q} + i0} \\ = \frac{E}{2q} \epsilon_q \frac{1}{(E - \epsilon_q)^2 - 4E_F \epsilon_q}; \quad (5)$$

where  $\epsilon_q = \epsilon^2 q^2 = 2m$  is electron dispersion,  $n_{1p}$  is the occupation of  $n = 1$  subband, and the factor 2 accounts for spin. From the pole position of  $\epsilon(E; q)$  at  $1 = V_{1212}(q)P_0(\epsilon_p; q)$ , we obtain the ISP dispersion law,

$$\epsilon_{p1}(q) = \epsilon_{p1}(0) + (\epsilon_q - \epsilon_0)E_F + (1 + \epsilon_q^{-1})\epsilon_q; \quad (6)$$

with  $\epsilon_{p1}(0) = \epsilon_0 + \epsilon_0 E_F$  and  $\epsilon_q = V_{1212}(q)$ , where  $V_{1212}(q)$  is defined by Eq. 1. The bottom of the ISP band is shifted up by  $\epsilon_0 E_F$  from the intersubband separation. Note, that the full depolarization shift includes also the Hartree renormalization of the intersubband separation, which has the same order of  $\epsilon_0 E_F$ . For parabolic QW this renormalization insures that  $\epsilon_{p1}(0) = \epsilon_0$  in accordance with the Kohn theorem [5, 13]. For relevant momenta  $q \ll 1$ , the  $q$ -dependence of the matrix elements,  $V_{ijkl}$ , can be neglected, which leads to quadratic ISP dispersion:  $\epsilon_{p1}(q) - \epsilon_{p1}(0) = q^2 = 2m_{p1}$ , where  $m_{p1} = m_0 = (1 + \epsilon_0)$  is the plasmon mass. Remarkably, for  $E_F = 1$ , the plasmon is much lighter than the electron,  $m_{p1} = m_0 - 1$ .

The ISP contribution to  $J$  comes from the region  $E > 2E_F - \epsilon_q + \epsilon_q$  of the  $(E; q)$  plane, where the

plasma is not Landau-damped. Then, for the plasma propagator,  $(E; q)$ , one has  $2\text{Im}(E; q) = 2A_q E \sim p_1(q)$ , with the oscillator strength,  $A_q$ , given by

$$A_q = \frac{V_{1212}(q) \frac{\partial P_0(E; q)}{\partial E}}{E - p_1(q)} = E_F \frac{q}{\frac{q}{2}} > 0; \quad (7)$$

Using the fact that  $q \ll 1$ , we can set  $q \approx 0$ . Then the joint spectral function (8) acquires a simple form

$$J_{p1} = 2 \frac{E_F}{2} \frac{q}{0} \frac{E_F}{2} \frac{q}{0} \frac{h}{2} \frac{1}{p_1(q)}; \quad (8)$$

where the  $\delta$ -function restricts the momenta to the domain where ISP is undamped.

The contribution Eq. (8) comes from the poles of in the integrand of Eq. (4). For conventional intersubband absorption, Fig. 2(a), the pole contribution carries almost the entire oscillator strength. By contrast, Eq. (8) yields only an additional contribution to the joint spectral function, whereas the main contribution comes from the numerators of  $P_0 = (1 - V_{1212}P_0)$  in Eq. (4). In calculating the latter, the denominators can be set to 1, i.e., ISPs are damped in the corresponding domain of the  $(E; q)$  plane. In other words, the main contribution,

$$J_{ee}(\omega; q) = \frac{\int \frac{dk_1 dk_2}{(2\pi)^4} n_{k_1} n_{k_2}}{8 \int \frac{dk_1 dk_2}{(2\pi)^4} n_{k_1} n_{k_2}}; \quad (9)$$

is due to excitation of two e-h pairs rather than plasmons and, being nonresonant, describes a broad plateau on which a sharp two-ISP peak resides.

Let us turn to the form of the two-electron matrix element  $M_q$ . Analytical expression, corresponding to the sum of the diagrams in Fig. 2(c), that describe possible channels of two-electron excitation, has the form

$$M_q = 2z_{12} \frac{V_{1222}(q) - V_{1211}(q)}{E_F + k_1 + q + k_2 + q - E_F - k_1 - k_2}; \quad (10)$$

Minus sign in Eq. (10) originates from the difference in energies of intermediate states for the two channels. Note, that the momenta of the final-state single-particle energies in the denominator of Eq. (10) are restricted by energy conservation  $\omega = E_F + k_1 + q + k_2 + q - E_F - k_1 - k_2$ . This relation ensures that the matrix element Eq. (10) depends only on the transferred momentum,  $q$ , so that

$$M_q = \frac{2z_{12}}{E_F} \frac{h}{V_{1222}(q) - V_{1211}(q)}; \quad (11)$$

Absorption coefficient | It is convenient to express the two-electron absorption coefficient,  $\alpha_2(\omega)$ , relative to the single-electron intersubband absorption,  $\alpha_1(\omega)$ . Namely, we introduce the ratio

$$\alpha_2(\omega) = \frac{P_2(\omega)}{P_1(\omega)} = \frac{J_2(\omega)}{J_1(\omega)}; \quad (12)$$

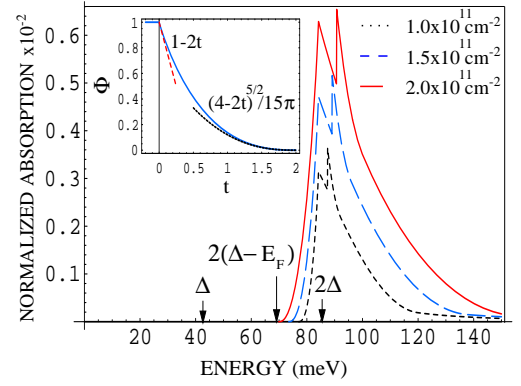


FIG. 3: Normalized two-electron absorption,  $\alpha_2$ , in  $d = 20$  nm GaAs QW is shown for applied bias  $U = 30$  meV and electron concentrations  $N = 1.0 \times 10^{11} \text{ cm}^{-2}$ ,  $1.5 \times 10^{11} \text{ cm}^{-2}$ , and  $2.0 \times 10^{11} \text{ cm}^{-2}$ . The right peak corresponds to two-plasma absorption. A row indicates the position of single-electron absorption peak at  $\omega_1$ . Inset: threshold behavior of two-electron absorption calculated from Eq. (15).

so that the area under the peak  $\alpha_2(\omega)$  is equal to the ratio of the corresponding oscillator strengths. To proceed further, we note that the difference,  $V_{1222}(q) - V_{1211}(q)$ , in the rhs of Eq. (11) has a general form  $\frac{2e^2 d}{\epsilon} f(qd)$ , where  $f(z)$  is a dimensionless function. Then the ISP contribution to  $\alpha_2$  can be presented as

$$\alpha_2(\omega) = \frac{4! E_F^2 r_s^2 m d^2}{(\omega - \omega_1)^2} [f(0)]^2; \quad (13)$$

where  $f(z) = \frac{2}{3E_F^2} \frac{R}{(2\pi)^2} J_{p1}(\omega; q)$  is a dimensionless function of  $\omega$ , and we assumed that  $q \ll 1$ . For ISP contribution this assumption is justified, since  $q \ll 0(k_F d)$ . Then, using Eq. (8), we obtain

$$\alpha_{p1} = \frac{0}{1 + 0} \frac{1}{\omega_1} \frac{2 p_1(0)}{\omega_1}; \quad (14)$$

where the width,  $\omega_{p1}$ , is given by  $\omega_{p1} = 2 \omega_1 (1 + 0) E_F$ . Note that  $p_1$  is non-zero only in the interval  $2 p_1(0) < \omega < 2 p_1(0) + \omega_{p1}$ . Since this width  $\omega_{p1} \ll E_F$ , we conclude that the plasma peak constitutes a sharp feature on top of a wider two-electron band in  $\alpha_2(\omega)$ .

The two-electron contribution to  $\alpha_2(\omega)$  can be naturally divided into two frequency domains. First domain corresponds to the photon energy  $\omega < 2 E_F$ , as illustrated in Fig. 1. In this domain we still have  $q \ll 1$ , so that Eq. (13) applies but with  $\omega_1$  calculated using  $J_{ee}(\omega; q)$ , defined by Eq. (9). Upon performing the  $q$ -integration, we obtain

$$t(\omega) = \frac{1}{2k_F^4} \int_{k_1, k_2 < k_F} dk_1 dk_2 \frac{k_1 k_2}{2k_F^2} t; \quad (15)$$

with  $t = (2 - \omega) E_F$ . The function  $t(\omega)$  evaluated numerically is plotted in Fig. 3 together with the asymptotes  $(1 - 2t)$  for  $t \ll 1$  and  $(4 - 2t)^{5/2}/15$  for

(2)  $t = 1$ . Singular points  $t = 2$  and  $t = 0$  correspond to excitation of two electrons from the bottom of the band and from the Fermi level, respectively. It follows from Eqs. (14) and (15), that the ratio of two-plasmon and two-electron contributions is equal to  $\phi(1 + \phi)^{-1} \approx 1$ .

In the second domain,  $\phi \approx 2$  &  $\phi \approx 0$ , two excited electrons have high energies. Thus, their momenta are almost opposite to each other, both having the absolute value of  $q_i = \frac{2m}{\hbar}(\omega - \frac{1}{2}) \approx \omega$ . Then the behavior of  $\sim_2(\omega)$  in the high-frequency domain is given by Eq. (13) with  $[f(0)]^2$  replaced by  $[f(qd)]^2$ . Thus, this behavior is determined by the actual confinement potential profile.

In the following we will consider the most common example of a biased rectangular QW.

**Biased rectangular QW** | Without bias, due to the QW symmetry, we have  $f(qd) = 0$  for all  $q$ . In the presence of bias  $U$ , which amounts to the perturbation  $Uz/d$  of confining potential, the size-quantization wave-functions in Eq. (1) acquire symmetry-breaking corrections,  $\psi_1(z) = \psi_1^{(0)}(z) + (Uz/d)\psi_2^{(0)}(z)$ , and  $\psi_2(z) = \psi_2^{(0)}(z) + (Uz/d)\psi_1^{(0)}(z)$ , where  $\psi_1^{(0)}, \psi_2^{(0)}$  are the size-quantization wave functions at  $U = 0$ , while the subband separation remains  $\approx \frac{3\pi^2}{2m} \frac{\hbar^2}{d^2}$ . Then a straightforward calculation yields  $f(qd) = \frac{Uz/d}{d} F(qd)$ , where the function  $F(s)$  can be expressed analytically and has the following behavior:  $F(0) = 595/144 \approx 4.13$ ;  $F(s) \sim \frac{1}{s^2}$ . Thus, the large- $\omega$  behavior of  $\sim_2(\omega)$  is the following:  $\sim_2(\omega) / \omega^2 \approx \frac{1}{\omega^2} \frac{1}{d^2}$ . This slow decay is illustrated in Fig. 3, where  $\sim_2(\omega)$ , calculated numerically for realistic parameters of quantum well, is plotted for three different electron concentrations. The relative oscillator strength for two-electron absorption is given by

$$\omega \sim_2(\omega) = C \frac{r_s E_F U}{2} \quad (16)$$

Using the explicit form of  $F(s)$  we have numerically cal-

culated the coefficient  $C$  in Eq. (16) to be  $8.2 \times 10^{-2}$ .

**Concluding remarks** | The lineshape of new peak is governed by three energy scales: sharp rise within the energy interval  $2E_F < \omega < 2E_F + \frac{3\pi^2}{2m} \frac{\hbar^2}{d^2}$ , slow decay for  $\omega > 2E_F + \frac{3\pi^2}{2m} \frac{\hbar^2}{d^2}$ , and a sharp two-ISP peak of the width  $\frac{3\pi^2}{2m} \frac{\hbar^2}{d^2} = \frac{1}{2} \frac{3\pi^2}{2m} \frac{\hbar^2}{d^2}$  on the top of the two-electron band. This difference in scales justifies the fact that we have disregarded the process of excitation of one ISP and one electron [this process is also captured by Eq. (4)]. The unusually small ISP contribution can be traced to the smallness of the ISP effective mass.

In general, the fact that a single photon can cause double ionization of an interacting system with a discrete spectrum (such as helium atom [14]) is known for almost four decades. A remarkable feature of quantum wells is that a sharp interaction-induced peak emerges in a system with continuous electron spectrum [15]. The necessary condition for observation of the two-electron absorption is that quantum well must be deep enough, namely deeper than  $7 \approx 3$ . Otherwise, two-electron absorption will result in photoionization. The above condition is always satisfied for thick quantum wells. However, increasing the thickness has a side effect that the number of size-quantization levels in the well increases, thus complicating the analysis of the absorption spectra. Note

namely, that although we considered the simplest model of homogeneous electron gas at zero temperature with two parabolic subbands, our theory can be easily generalized to the realistic situations [16, 17, 18, 19]. Important is that nonparabolicity, finite temperature, disorder, etc. are not expected to suppress the two-electron absorption.

**ACKNOWLEDGEMENTS** | M.E.R. acknowledges support by NSF under Grant No. DMR-0503172. T.V.S. acknowledges support by NSF under Grant No. DMR-0305557 and by ARL under Grant No. DAAD19-01-2-0014.

- 
- [1] K.K. Choi, *The Physics of Quantum Well Infrared Photodetectors* (World Scientific, Singapore, 1997).  
 [2] *Intersubband Transitions in Quantum Wells: Physics and Device Application I*, edited by H.C. Liu and F. Capasso (Academic Press, San Diego, 2000).  
 [3] T. Ando, *Phys. B: Condens. Matter* **26**, 263 (1977).  
 [4] T. Ando, A.B. Fowler, and F. Stern, *Rev. Mod. Phys.* **54**, 437 (1982).  
 [5] L. Breiy, N.F. Johnson, and B.I. Halperin, *Phys. Rev. B* **40**, 10647 (1989).  
 [6] C.A. Ullrich, and G. Vignale, *Phys. Rev. Lett.* **87**, 037402 (2001).  
 [7] S.V. Fal'eev and M.I. Stockman, *Phys. Rev. B* **66**, 085318 (2002).  
 [8] J. Li, and C.Z. Ning, *Phys. Rev. Lett.* **91**, 097401 (2003).  
 [9] I.W. Akimuller et al., *Phys. Rev. B* **69**, 205307 (2004).  
 [10] M.F. Pereira, S.-C. Lee, and A. Wacker, *Phys. Rev. B* **69**, 205310 (2004).  
 [11] J. Li and C.Z. Ning, *Phys. Rev. B* **70**, 125309 (2004).  
 [12] M. Kira and S.W. Koch, *Phys. Rev. Lett.* **93**, 076402 (2004).  
 [13] L. Breiy et al., *Phys. Rev. B* **42**, 1240 (1990).  
 [14] T.A. Carlson, *Phys. Rev.* **156**, 142 (1967).  
 [15] For interaction-assisted intrasubband absorption, which is due to pairs of low-energy excitations, the absorption coefficient turns to zero in the long wavelength limit, see, e.g., R.N. Ifossi, S. Conti, and M.P. Tosi, *Phys. Rev. B* **58**, (1998); E.G. Mishchenko, M.Yu. Reizer, and L.I. Glazman, *Phys. Rev. B* **69**, 195302 (2004), and references therein.  
 [16] D.E. Nikonov et al., *Phys. Rev. Lett.* **79**, 4633 (1997).  
 [17] A.G.U. Perera et al., *Appl. Phys. Lett.* **72**, 1596 (1998).  
 [18] M.F. Pereira and H. Wenzel, *Phys. Rev. B* **70**, 205331 (2004).  
 [19] D.C. Larabee et al., *Appl. Phys. Lett.* **83**, 3936 (2003).